Perturbative hypernetted-chain equation for mixtures: Applications to Coulomb plasma and H_2+H mixtures

Hong Seok Kang
Department of Chemistry and New Materials, College of Science and Engineering, Jeonju University, Hyoja-dong, Wansan-ku, Chonju, Chonbuk, Korea 560-759

Francis H. Ree
Lawrence Livermore National Laboratory, University of California, Livermore, California 94551
(Received 11 November 1997)

The perturbative hypernetted-chain equation for one-component systems [J. Chem. Phys. **103**, 9377 (1995)] has been extended to mixture systems by approximating the bridge function of a system by that of a reference system whose repulsive range is chosen to satisfy thermodynamic consistency of partial isothermal compressibilities for individual components in a mixture. Applications to strongly coupled Coulomb and Yukawa mixtures and $H+H_2$ mixtures show that the theory provides radial distribution functions and thermodynamic functions that are in close agreement with exact computer-simulation data, some of which are obtained in this work. They are often superior to or at least comparable to the best available theories in the literature. [S1063-651X(98)13905-3]

PACS number(s): 52.25.−b, 05.70.−a

I. INTRODUCTION

Integral equations for the pair-correlation functions have been used very successfully in the study of equilibrium properties of dense fluids. The present work focuses on the perturbative hypernetted-chain (PHNC) equation [1,2], in which the bridge function for a system of interest is replaced by that of a reference system with a density-dependent pair potential, and aims toward extending our earlier work for a single-component system to mixtures. For this, we introduce a more sophisticated choice of the reference system, as will be described in the next section.

In Sec. III we apply the present theory to plasma mixtures interacting with either an unscreened or a screened Coulomb potential to compare with the best available theory, i.e., Rosenfeld's density-functional theory (DFT) [3]. The DFT gives the internal energy within a three to five figure accuracy of Monte Carlo data [4–6] for unscreened mixtures. We next apply the present theory to a H_2+H mixture to compute thermodynamic properties and radial distribution functions. The results are compared with Monte Carlo data and those from another successful theory of dense fluids, i.e., the HMSA equation of Zerah and Hansen [7,8].

II. FORMULATIONS

The PHNC integral equation for a multicomponent mixture employs a closure relation

$$B_{ij}(r)=B_{ij,0}(r), \tag{2.1}$$

where $B_{ij}(r)$ and $B_{ij,0}(r)$ denote the bridge functions between species i and j for a system of interest and those for a reference system, respectively. The PHNC chooses the range (λ_{ij}) of the reference potential $V_{ij,0}(r)$ to depend on temperature T and density ρ. For a one-component system, a choice of $\lambda=\min(a_{\rm fcc},r^*)$ gives reliable results. Here, $a_{\rm fcc}(=2^{1/6}/\rho^{1/3})$ is the nearest-neighbor distance for the face-centered-cubic lattice and r^* is the interatomic distance where $V(r)$ is at the minimum.

For a mixture, λ_{ij} can be different for a different (i,j) pair. In this work, we choose λ_{ij} $(i\neq j)$ to be additive, i.e., $\lambda_{ij}=(\lambda_{ii}+\lambda_{jj})/2$. λ_{ii} is chosen so that the partial isothermal compressibility $\partial(\beta P)/\partial\rho_i$, from the compressibility relation

$$\frac{\partial(\beta P)}{\partial\rho_i}=1-\rho\sum_j x_j\int d\mathbf{r}\; c_{ij}(r), \tag{2.2}$$

gives the same result as that obtained by numerical differentiation $\partial(\beta P)/\partial\rho_i$ of the virial equation

$$\frac{\beta P}{\rho}=1-\frac{\beta\rho}{6}\sum_{i,j} x_i x_j\int d\mathbf{r}\; g_{ij}(r) r\,\frac{dV_{ij}(r)}{dr}. \tag{2.3}$$

Here $\beta=1/kT$ ($k=$ the Boltzmann constant) and $c_{ij}(r)$ is the direct correlation function. For a plasma system with a compensating background of opposite charge, Eqs. (2.2) and (2.3) need to be modified to include the background contributions. This is done by replacing $c_{ij}(r)$ and $g_{ij}(r)$ by $c_{ij}(r)+\beta V_{ij}(r)$ and $g_{ij}(r)-1$, respectively.

For a given λ_{ij}, a pair potential is divided into two parts. Namely,

if $\lambda_j<r_{ij}^*$,

$$V_{ij,1}(r)=V_{ij}(\lambda_{ij})-V'_{ij}(\lambda_{ij})(\lambda_{ij}-r), \qquad \text{if } r\leqslant\lambda_{ij},$$

$$=V_{ij}(r), \qquad \text{if } r>\lambda_{ij}, \tag{2.4}$$

$$V_{ij,0}(r)=V_{ij}(r)-V_{ij,1}(r); \tag{2.5}$$

TABLE I. Comparison of the excess internal energy for the TCP: the Monte Carlo data [4–6], the PHNC (this work), and Rosenfeld's DFT [3]. Z_2 is the ionic charge of species 2 ($Z_1=1$); $\Gamma_e=(e^2/a_e kT)$, where a_e is the electron sphere radius; and x is the mole fraction of species 2.

			βU^e		
Z_2	Γ_e	x	Exact	PHNC	DFT
3	10	0.01	−8.458 74±0.000 11	−8.4543	−8.4628
	10	0.02	−8.919 27±0.000 11	−8.9152	−8.934
	10	0.05	−10.300 53±0.000 14	−10.2975	−10.297
	10	0.1	−12.602±0.001	−12.601	−12.592
	10	0.2	−17.208±0.001	−17.207	−17.201
	10	0.5	−31.035±0.002	−31.027	−31.032
	15	0.05	−15.790 68±0.000 26	−15.7847	−15.7850
	15	0.1	−19.265±0.001	−19.260	−19.252
	15	0.2	−26.212±0.001	−26.209	−26.199
	15	0.5	−47.066±0.002	−47.055	−47.057
	20	0.01	−17.601 88±0.000 26	−17.5904	−17.6033
	20	0.05	−21.318 34±0.000 19	−21.3105	−21.3100
	20	0.1	−25.963±0.001	−25.959	−25.948
	20	0.2	−35.260±0.002	−35.255	−35.237
	20	0.5	−63.145±0.002	−63.137	−63.126
5	10	0.01	−9.204 14±0.000 15	−9.2022	−9.2033
	10	0.05	−14.027 53±0.000 15	−14.0331	−14.0081
	10	0.1	−20.058 40±0.000 17	−20.0682	−20.0301
	10	0.2	−32.123 99±0.000 23	−32.1357	−32.0974
	10	0.5	−68.339 13±0.000 32	−68.3421	−68.3609
8	10	0.01	−10.756 98±0.000 18	−10.7617	−10.7466

if $\lambda_j \geq r_{ij}^*$,

$$V_{ij,0}(r)=V\left(\frac{r_{ij}^*}{\lambda_{ij}}\,r\right)-V(r_{ij}^*), \tag{2.6}$$

$$V_{ij,1}(r)=V_{ij}(r)-V_{ij,0}(r). \tag{2.7}$$

Equations (2.4) and (2.5) represent a direct extension of the method used for the one-component case [1,2] to a mixture. In this work, we introduce an additional perturbation scheme via Eqs. (2.6) and (2.7) when $\lambda_{ij} \geq r_{ij}^*$. They ensure that $V_{ij,0}(r)$ is a continuous function of λ_{ij} at a given r. As will be shown below, this scheme allows the aforementioned thermodynamic consistency to be fulfilled even at low density, where $a_{\rm fcc} > r_{ij}^*$. Note that this choice does not affect calculations for purely repulsive potentials, since r_{ij}^* occurs at infinity.

Once the reference potential is defined, $B_{ij,0}(r)$ is determined by solving the Ornstein-Zernike relation with Ballone *et al.*'s closure relation [9]

$$B_{ij,0}(r)=[1+s\,\gamma_{ij,0}(r)]^{1/s}-1-\gamma_{ij,0}(r), \tag{2.8}$$

where $s=15/8$ and $\gamma_{ij,0}(r)$ is the indirect correlation function. In summary, we solve Eqs. (2.1)–(2.8) by an iterative cycle until a self-consistent solution is obtained.

III. RESULTS AND DISCUSSION

The two-component plasma (TCP) corresponds to the simplest model of plasma mixtures where ions with charges Z_1 and Z_2 (in units of e) move in a uniform background. Parameters describing this system are the plasma coupling parameter $\Gamma=e^2/(kTa)$, Z_1, Z_2, and mole fraction x of species 2, where $a(=3/4\pi\rho)^{1/3}$ is the ion-sphere radius. An alternative description is possible in terms of $\Gamma_e=e^2/(kTa_e)$ instead of Γ, where $a_e(=3/4\pi\rho_e)^{1/3}$ is the electron radius and ρ_e is the electron density.

Table I compares the excess internal energy U^e calculated from the PHNC with those from computer simulations [4–6] and the DFT [3] for the TCP with $Z_1=1$ and $Z_2>Z_1$. The PHNC is generally superior to the DFT at $x>0.01$. We also note that the present PHNC gives better results compared to a simpler version of the theory that does not use the self-consistency criterion for λ_{ij}. For example, the use of $\lambda_{11}=\lambda_{12}=\lambda_{22}=a_{\rm fcc}$ gives $\beta U^e=-68.1143$ at $\Gamma_e=10$, $Z_2=5$, and $x=0.5$, compared with Monte Carlo ($=-68.339\,13$) and PHNC ($=-68.3421$) data in Table I. Yet, detailed calculations show that deviations of U^e from those predicted by the so-called ''linear mixing rule'' [10,11] are not accurately predicted by the refined PHNC. This is related to the fact that the law is so accurate that the deviation from it is generally very small, i.e., 0.06% or less. A similar situation also occurs for the DFT. Figure 1 shows that the PHNC also gives accurate partial radial distribution functions $g_{ij}(r)$, which are at least as accurate as the DFT. See Fig. 5 of Ref. [3].

Next, we briefly describe results of the PHNC calculations for the Yukawa system, which is a more realistic model for plasma than the one-component plasma (OCP) or the TCP. For a two-component Yukawa mixture composed of ions with charges Z_1 and Z_2, an interaction potential be-

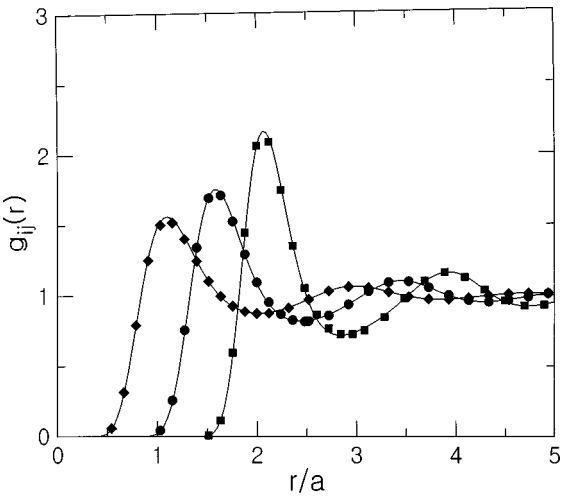

FIG. 1. Radial distributions $g_{ij}(r)$ for an equimolar TCP mixture with $Z_1=1$ and $Z_2=5$ at $\Gamma_e=10$. Diamonds, circles, and squares represent the Monte Carlo data of DeWitt, Slattery, and Chabrier [12] for the 11, 12, and 22 interactions, respectively. Solid lines correspond to the PHNC.

tween (i,j) ions is given by $\beta V_{ij}(r)=Z_iZ_j\Gamma e^{-\kappa r}/r$, where distance r is in units of a. The potential energy of this system depends on five parameters: Γ, Z_1, Z_2, x, and κ. Although not shown here, the PHNC can predict the excess internal energy of the one-component Yukawa system with an accuracy similar to that for the OCP in the range of $\kappa \leqslant 2$. This was confirmed by comparing the PHNC calculations with recent Monte Carlo data of Hamaguchi and coworkers [13]. In addition, we have found that λ, which satisfies the self-consistency criterion, lies very close to $a_{\rm fcc}$ at all κ values investigated near the freezing line. Typically, differences between the two are within 5%. This is somewhat unexpected in that the weakly screened Yukawa system freezes into the body-centered-cubic lattice [14].

Table II gives a comparison of the potential energy between Yukawa charges (U^{pp}) calculated from the PHNC and the hypernetted chain approximation (HNC) for the two-component Yukawa system. Also shown are results from the Yukawa mixing rule (YMR) [15] based on the calculations performed on the one-component Yukawa systems using the PHNC or the HNC. Here U^{pp} is related to the linear response energy $U_{\rm lin.resp.}$ by

$$\beta U_{\rm lin.resp.}=\beta U^{pp}-3\Gamma\frac{\langle Z\rangle^2}{2\kappa^2}-\frac{\Gamma}{2}\langle Z^2\rangle\kappa \tag{3.1}$$

$$=\frac{3\Gamma}{4\pi^2}\sum_{i,j}x_ix_jZ_iZ_j\int dk\; h_{ij}(k)\frac{k^2}{k^2+\kappa^2}$$

$$-\frac{\Gamma}{2}\langle Z^2\rangle\kappa, \tag{3.2}$$

where the distance is in units of the ion-sphere radius a [15]. The YMR can be expressed in terms of $u^{pp}(\equiv\beta U^{pp})$ by

$$u^{pp}(Z_1,Z_2,\Gamma,x,\kappa)=(1-x)u_1^{pp}(\Gamma_1,\kappa_1)+xu_2^{pp}(\Gamma_2,\kappa_2), \tag{3.3}$$

where u_i^{pp} denotes the reduced potential energy between Yukawa charges in the one-component system of species i, and

$$\Gamma_i=(Z_i^2/R_i)\Gamma,\quad \kappa_i=\kappa R_i\,. \tag{3.4}$$

Here, R_i is the solution of the coupled algebraic equations

$$R_i=\frac{Z_iY(\kappa R_i)}{(1-x)Z_1Y(\kappa R_1)+xZ_2Y(\kappa R_2)}\quad (i=1,2), \tag{3.5}$$

and

$$Y(t)=\frac{2t^3}{3[e^t(t-1)+e^{-t}(t+1)]}. \tag{3.6}$$

TABLE II. Potential energy U^{pp} between Yukawa charges calculated from the PHNC and the HNC at different compositions and the screening parameter κ at $\Gamma=20$, $Z_1=1$, and $Z_2=3$. x denotes the mole fraction of ionic species 2. $\Gamma_{\rm eff}$ is the effective coupling parameter. Also shown are the results from the Yukawa mixing rule (YMR). PHNC-YMR denotes the data based on the YMR using the PHNC for one-component systems. A similar definition applies to HNC-YMR. See the text for more detail.

			βU^{pp}			
x	κ	$\Gamma_{\rm eff}$	PHNC	PHNC-YMR	HNC	HNC-YMR
0.1	0.4	21.73	248.837	248.842	249.029	249.023
	0.6	17.81	101.553	101.558	101.742	101.736
	0.8	14.60	51.4435	51.4484	51.6277	51.6225
	1.0	11.97	29.2327	29.2370	29.4107	29.4057
0.2	0.4	30.74	337.295	337.301	337.555	337.546
	0.6	25.19	137.045	137.051	137.300	137.292
	0.8	20.66	69.0293	69.0361	69.2779	69.2697
	1.0	16.94	38.9594	38.9654	39.1990	39.1911
0.5	0.4	61.17	688.223	688.234	688.695	688.687
	0.6	50.11	279.248	279.253	279.707	279.699
	0.8	41.05	140.237	140.237	140.683	140.675
	1.0	33.64	78.7460	78.7468	79.1764	79.1688

TABLE III. Comparison of the compressibility factor $\beta P/\rho$ and the excess internal energy U^e of an equimolar $H+H_2$ mixture: Exact data (the exact data with standard deviations inside parentheses are from the Monte Carlo simulations performed in this work using $10^6 \sim 2\times 10^6$ configurations, while values without standard deviations are taken from Ref. [8]), the PHNC, and the HMSA [8]. Also shown are data on the zero wave-vector limit of the Bhatia-Thornton structure factor $S_{cc}(0)$ based on the PHNC. $S_{cc}(0)$ was divided by that for an ideal mixture to better describe the tendency for a phase separation. x denotes the mole fraction of H_2. See the text for more detail.

		$\beta P/\rho$			βU^e			$\frac{S_{cc}(0)}{(1-x)x}$
T (K)	ρ (Å^{-3})	Exact	PHNC	HMSA	Exact	PHNC	HMSA	
1000	0.002 06	1.034(7)	1.034		0.0067(1)	0.0068		0.990
	0.02	1.434(1)	1.434		0.1043(1)	0.1039		0.889
	0.06	3.123	3.124	3.110	0.675	0.674	0.664	0.620
	0.2	16.996(6)	17.086	17.053	7.518(4)	7.540	7.538	0.137
5000	0.002 06	1.020(1)	1.020		0.008 80(9)	0.008 74		1.040
	0.02	1.215(1)	1.216		0.0977(6)	0.0979		0.921
	1.0	35.31	35.32	35.37	24.07	24.09	24.17	0.052
10 000	0.002 06	1.014(1)	1.014		0.007 36(6)	0.007 36		1.028
	0.02	1.148(1)	1.148		0.0788(3)	0.0787		0.934
	0.2	3.212	3.212	3.214	1.309	1.308	1.307	0.476
	1.0	18.410(1)	18.429	18.443	12.536(2)	12.548	12.549	0.096

Since computer-simulated data are not available for this system, it is difficult to assess the accuracy of the PHNC. However, Table II shows that the YMR holds very well for both of the PHNC and the HNC in the strongly coupled regime. In fact, the smallest value of the effective coupling parameter $\Gamma_{\rm eff}(=\{(1-x)\Gamma_1+x\Gamma_2\}e^{-\kappa})$ is 11.97. We also note that deviation of the PHNC data from that predicted by the YMR is generally negative, while the opposite is the case for the HNC.

Table III shows that the PHNC is also reliable for a $H+H_2$ mixture interacting with Morse potentials. To test this, we made additional Monte Carlo simulations. We note that the present theory is slightly superior to the HMSA [8] (the potential parameters used in this work are the same as those in Ref. [8]). Figures 2 and 3 render further support to the good performance of the PHNC. At $T=5000$ K and $\rho=1$ Å^{-3}, the first peaks in the H_2-H_2 radial distribution function $g_{22}(r)$ are 1.798 ± 0.005, 1.802, 1.69, and 1.72 for the Monte Carlo data obtained in this work, the PHNC, and the one- and two-parameter HMSA, respectively. (See Fig. 2.) However, the corresponding peak for the H-H radial distribution function $g_{11}(r)$ is not accurately predicted. (The two-parameter HMSA determines parameters in ''switching functions'' by imposing a condition of thermodynamic consistency between two partial compressibilities similar to the one used here. The switching functions mix the soft mean-spherical approximation at small r and the HNC closure at

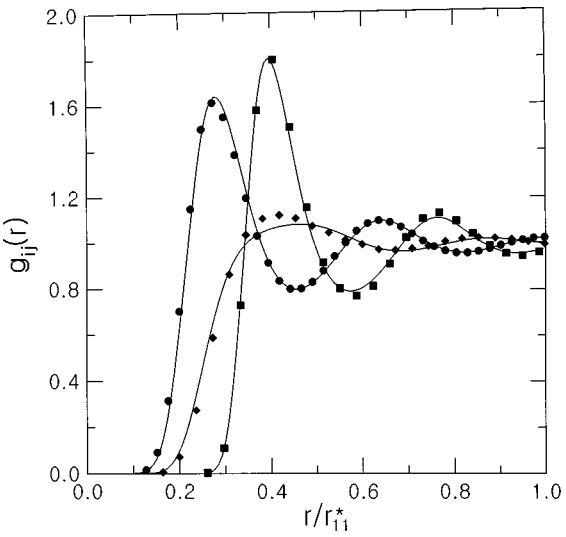

FIG. 2. Radial distributions $g_{ij}(r)$ for an equimolar mixture of atomic (=species 1) and molecular (=species 2) hydrogen at $T=5000$ K and $\rho=1$ Å^{-3}. Diamonds, circles, and squares correspond to the Monte Carlo data (obtained in this work) for the 11, 12, and 22 interactions, respectively. Solid lines represent the PHNC.

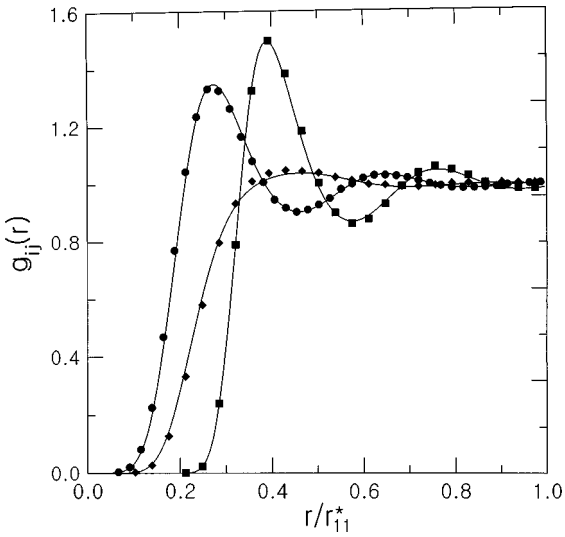

FIG. 3. Radial distributions $g_{ij}(r)$ for an equimolar mixture of atomic (=species 1) and molecular (=species 2) hydrogen at $T=10\,000$ K and $\rho=1$ Å^{-3}. Notations are the same as in Fig. 2.

large r. On the one hand, the one-parameter HMSA employs a single switching function whose parameter is determined from the consistency of the total compressibility.) Note that the system has a very strong tendency for heterocoordination at this temperature and density. This can be seen by the zero wave-vector limit of the normalized Bhatia-Thornton (BT) structure factor [16] $S_{cc}(0)/x(1-x)$ predicted by the PHNC. The term $x(1-x)$ predicted by the PHNC. The term $x(1-x)$ in the denominator describes the contribution by an ideal mixture, where $x=1-x_1$ is the mole fraction of the species 2. The BT structure factor is defined by

$$S_{cc}(k)=N\langle C^*(k)C(k)\rangle, \tag{3.7}$$

where

$$C(k)=[x_2N_1(k)-x_1N_2(k)]/N, \tag{3.8}$$

$$N_i(k)=\sum_j^{N_i} \exp(i\mathbf{k}\cdot\mathbf{R}_j). \tag{3.9}$$

Here, $N=N_1+N_2$ is the total number of particles, and $S_{cc}(0)$ is related to the Gibbs free energy G of the system by $S_{cc}(0)=kT/(\partial^2 G/\partial x^2)_{P,T,N}$. Therefore, $S_{cc}(0)\sim 0$ implies that the system has a strong tendency for compound formation between unlike pairs. We observe that partial radial distribution functions calculated from the PHNC are in better agreement with Monte Carlo data when $S_{cc}(0)$ becomes larger. Figure 3 shows that this is actually the case when $T=10\,000$ K and $\rho=1.0$ Å^{-3}. Table III also shows that the PHNC actually yields a solution (which satisfies the thermodynamic consistency) at all temperatures and densities investigated, even at a low density ($\rho=0.002\,06$ and 0.02 Å^{-3}), for which $a_{\rm fcc}>r_{ij}^*$ for all (i,j) pairs. This is not possible without the use of $V_{ij,0}(r)$ given in Eq. (2.6).

IV. CONCLUSION

We have extended the perturbative hypernetted-chain equation recently developed for the single-component systems to mixtures and have successfully applied it to two entirely different mixtures, i.e., plasma mixtures and $H+H_2$ mixtures. Furthermore, we have shown that the new PHNC is applicable to mixtures at wide temperature and density. We expect that the PHNC will be useful for the study of liquid metals and alloys when combined with a suitable pseudopotential theory.

ACKNOWLEDGMENTS

The work of H. S. Kang was supported by a grant from Jeonju University. The work of Francis H. Ree was done under the auspices of the U.S. Department of Energy by Lawrence Livermore National Laboratory under Contract No. W-7405-ENG-48.

[1] H. S. Kang and F. H. Ree, J. Chem. Phys. **103**, 3629 (1995).
[2] H. S. Kang and F. H. Ree, J. Chem. Phys. **103**, 9370 (1995).
[3] Y. Rosenfeld, Phys. Rev. E **54**, 2827 (1996).
[4] S. Ogata, H. Iyetomi, S. Ichimaru, and H. M. Van Horn, Phys. Rev. E **48**, 1344 (1993).
[5] *Strongly Coupled Plasma Physics*, edited by W. Kraeft and M. Schlanges (World Scientific, Singapore, 1996).
[6] H. E. DeWitt, W. L. Slattery, and G. Chabrier, Physica B **228**, 21 (1996).
[7] G. Zerah and J. P. Hansen, J. Chem. Phys. **84**, 2336 (1986); J. P. Hansen and G. Zerah Phys. Lett. A **108**, 277 (1985).
[8] D. Levesque, J. J. Weis, and G. Chabrier, J. Chem. Phys. **94**, 3096 (1991).
[9] P. Ballone, G. Pastore, G. Galli, and D. Gazzillo, Mol. Phys. **59**, 275 (1986).
[10] J. P. Hansen, G. M. Torrie, and P. Vieillefosse, Phys. Rev. A **16**, 2153 (1977).
[11] B. Brami, J. P. Hansen, and F. Joly, Physica A **95**, 505 (1979).
[12] H. E. DeWitt (private communication).
[13] R. T. Farouki and S. Hamaguchi, J. Chem. Phys. **101**, 9885 (1994); S. Hamaguchi, R. T. Farouki, and D. H. E. Dubin, Phys. Rev. E **56**, 4671 (1997).
[14] K. Kremer, M. O. Robbins, and G. S. Grest, Phys. Rev. Lett. **57**, 2694 (1986).
[15] Y. Rosenfeld, Phys. Rev. E **47**, 2676 (1993).
[16] A. B. Bhatia and D. E. Thornton, Phys. Rev. B **2**, 3004 (1970).